Available online at www.eccomasproceedia.org
Eccomas Proceedia SMART (2023) 659-670

ECCOMAS
Proceedia

X ECCOMAS Thematic Conference on Smart Structures and Materials
SMART 2023
D.A. Saravanos, A. Benjeddou, N. Chrysochoidis and T. Theodosiou (Eds)

PARAMETRIC MODEL ORDER REDUCTION FOR PARAMETER IDENTIFICATION OF ADAPTIVE HIGH-RISE STRUCTURES

Manuel Vierneisel*, Amelie Zeller†, Spasena Dakova†, Michael Böhm†, Oliver Sawodny† and Peter Eberhard*

*Institute of Engineering and Computational Mechanics
University of Stuttgart
Pfaffenwaldring 9, 70569 Stuttgart, Germany
{manuel.vierneisel, peter.eberhard}@itm.uni-stuttgart.de
www.itm.uni-stuttgart.de

† Institute for System Dynamics
University of Stuttgart
Waldburgstraße 17/19, 70563 Stuttgart, Germany
{amelie.zeller, spasena.dakova, michael.boehm, oliver.sawodny}@isys.uni-stuttgart.de
www.isys.uni-stuttgart.de

Key words: parametric modeling, model order reduction, parameter identification

Abstract. The building sector is one of the largest contributors to global carbon dioxide emissions and resource consumption. One promising way to save resources is to build adaptive buildings, that are equipped with sensors, actuators, and a control-unit to counteract deformations and vibrations caused by external loads. The first adaptive high-rise building was built on the campus of the University of Stuttgart within the framework of the Collaborative Research Center 1244. This contribution proposes a parametric reduced order model suitable for an efficient parameter identification. In a first step a sensitivity analysis is conducted to identify the most influential parameters on the system behavior. Different parametric model order reduction techniques are then investigated such that the size of the reduced system matrices is as small as possible on the one hand and the approximation error between the reduced order model and the full order model in the parameter, time, and frequency domain is minimized on the other hand. Compared to classical model updating routines, this parameterized reduced order model requires much lower online computational effort since it is not necessary to calculate the system matrices and perform a model order reduction in each iteration step of the parameter identification.

1 INTRODUCTION

The building sector is a significant contributor to global carbon dioxide emissions and resource consumption, see [1]. Adaptive buildings are a promising way to reduce emissions and improve energy efficiency. The Collaborative Research Center 1244 (SFB 1244) "Adaptive Skins and Structures for the Built Environment of Tomorrow" at the University of Stuttgart works on adaptive facades that are able to react on different weather conditions as well as adaptive bearing structures of buildings that can react

Peer-review under responsibility of the organizing committee of SMART 2023.
doi: 10.7712/150123.9820.443871

on vibrations caused by external loads such as wind loads with the help of sensors and actuators. In [2] an overview of the current research work is provided. The first adaptive high-rise building worldwide is built at the University of Stuttgart and serves to test the developed concepts. The building is equipped with multiple sensor systems and actuators for state monitoring and active disturbance compensation. In order to apply those state estimation and control algorithms during the operation phase, an accurate mathematical model of the building is required. Model updating methods make it possible to identify parameters so that the system behavior of the model matches the real system behavior as closely as possible.

The main contribution of this work is the development of a parameterized reduced order model which is then used for an efficient parameter identification, where the system has to be evaluated multiple times with different parameters. The parameterization allows a very efficient evaluation of the system matrices at specific parameter points during repeated iteration steps. In the online phase of the parameter identification process, there is no need to recompute the reduced order model or to evaluate the full order model as the reduction of the system dimension is already done in the offline phase.

This contribution is structured as follows. Section 2 explains the theoretical basis of linear and parametric model order reduction as well as the used error measures. The modeling of the adaptive building and the parameterization is presented in Section 3. Afterwards, Section 4 outlines parametric model order reduction of the adaptive structure and discusses the obtained results. Finally, a conclusion is given in Section 5.

2 THEORETICAL BACKGROUND

This section explains, how to mathematically describe the system dynamics of mechanical systems. Furthermore, the theoretical foundations of model order reduction and parametric model order reduction are introduced and error measures applied in this contribution are defined.

2.1 System description

The linear finite element method as described in [3, 4] is a widespread method to compute the behavior of structural mechanical systems. The resulting system is described by a second order linear differential equation

$$\begin{aligned} \boldsymbol{M}\ddot{\boldsymbol{q}}(t) + \boldsymbol{D}\dot{\boldsymbol{q}}(t) + \boldsymbol{K}\boldsymbol{q}(t) = \boldsymbol{B}\boldsymbol{u}(t), \qquad & \boldsymbol{q}(0) = \boldsymbol{q}_0,\ \dot{\boldsymbol{q}}(0) = \dot{\boldsymbol{q}}_0,\ t \geq 0, \\ \boldsymbol{y}(t) = \boldsymbol{C}\boldsymbol{q}(t), & \end{aligned} \tag{1}$$

which is also called equation of motion. Herein, $\boldsymbol{q}(t) \in \mathbb{R}^N$ is the vector of node displacements and rotations with in total N degrees of freedom and $\dot{\boldsymbol{q}}(t)$ and $\ddot{\boldsymbol{q}}(t)$ are its corresponding first and second derivatives with respect to time $t \in \mathbb{R}_{\geq 0}$. In addition, $\{\boldsymbol{M}, \boldsymbol{D}, \boldsymbol{K}\} \in \mathbb{R}^{N \times N}$ are the mass, damping, and stiffness matrices, respectively. The matrix $\boldsymbol{B} \in \mathbb{R}^{N \times r}$ maps the inputs $\boldsymbol{u} \in \mathbb{R}^r$ to the node displacements and the matrix $\boldsymbol{C} \in \mathbb{R}^{o \times N}$ describes the relation between the node displacements and the outputs $\boldsymbol{y}(t) \in \mathbb{R}^o$. By introducing the angular frequency $\omega \in \mathbb{R}$ and the imaginary unit i and applying a Fourier transformation to Equation (1), the frequency response function

$$\boldsymbol{H}(\mathrm{i}\omega) = \boldsymbol{C}\left(-\omega^2\boldsymbol{M} + \mathrm{i}\omega\boldsymbol{D} + \boldsymbol{K}\right)^{-1}\boldsymbol{B} \quad \in \mathbb{C}^{o \times r} \tag{2}$$

is derived, which describes the input to output behavior in the frequency domain.

2.2 Model order reduction

In many applications, a very fine finite element mesh is required to obtain reasonable results. The resulting large system matrices lead to high numerical complexity and consequently long computation times for e.g. eigenvalue analysis or transient simulations. Projection-based model order reduction is one way to overcome this problem, see e.g. [5, 6, 7]. The nodal displacements are approximated by a projection into a lower dimensional subspace $\mathcal{V}$ with

$$\boldsymbol{q}(t) \approx \boldsymbol{V}\boldsymbol{q}_{\mathrm{red}}(t), \tag{3}$$

where $\boldsymbol{V} \in \mathbb{R}^{N\times n}$ with $n \ll N$ is the projection matrix and $\boldsymbol{q}_{\mathrm{red}}(t) \in \mathbb{R}^n$ are the reduced coordinates. The key challenge is the trade-off between a sufficiently low dimensional subspace for efficient computation and a good approximation of the dynamic behavior of the system. Combining the Equations (3) and (1) and applying an orthogonal Galerkin projection results in the reduced order equation of motion

$$\begin{aligned} \underbrace{\boldsymbol{V}^{\mathsf{T}}\boldsymbol{M}\boldsymbol{V}}_{\boldsymbol{M}_{\mathrm{red}}}\ddot{\boldsymbol{q}}_{\mathrm{red}}(t) + \underbrace{\boldsymbol{V}^{\mathsf{T}}\boldsymbol{D}\boldsymbol{V}}_{\boldsymbol{D}_{\mathrm{red}}}\dot{\boldsymbol{q}}_{\mathrm{red}}(t) + \underbrace{\boldsymbol{V}^{\mathsf{T}}\boldsymbol{K}\boldsymbol{V}}_{\boldsymbol{K}_{\mathrm{red}}}\boldsymbol{q}_{\mathrm{red}}(t) &= \underbrace{\boldsymbol{V}^{\mathsf{T}}\boldsymbol{B}}_{\boldsymbol{B}_{\mathrm{red}}}\boldsymbol{u}(t), \\ \bar{\boldsymbol{y}}(t) &= \underbrace{\boldsymbol{C}\boldsymbol{V}}_{\boldsymbol{C}_{\mathrm{red}}}\boldsymbol{q}_{\mathrm{red}}(t) \end{aligned} \tag{4}$$

with the reduced system matrices $\{\boldsymbol{M}_{\mathrm{red}}, \boldsymbol{D}_{\mathrm{red}}, \boldsymbol{K}_{\mathrm{red}}\} \in \mathbb{R}^{n\times n}$, $\boldsymbol{B}_{\mathrm{red}} \in \mathbb{R}^{n\times r}$ and $\boldsymbol{C}_{\mathrm{red}} \in \mathbb{R}^{o\times n}$ as well as the output $\bar{\boldsymbol{y}}(t) \in \mathbb{R}^o$ calculated with the reduced system. Replacing the full order system matrices in Equation (2) with the reduced order system matrices gives the frequency response function $\bar{\boldsymbol{H}}(\mathrm{i}\omega) \in \mathbb{C}^{o\times r}$ calculated with the reduced system matrices. Both, $\boldsymbol{H}(\mathrm{i}\omega)$ and $\bar{\boldsymbol{H}}(\mathrm{i}\omega)$ have the same dimensions.

Plenty of methods exist to obtain the reduction matrix $\boldsymbol{V}$. The modal truncation approach uses the first n eigenmodes as the columns of the projection matrix $\boldsymbol{V} = [\boldsymbol{\varphi}_1\ \boldsymbol{\varphi}_2\ \ldots\ \boldsymbol{\varphi}_n]$. Another method is moment matching using Krylov subspaces. It matches the transfer function of the full order and the reduced order model $\boldsymbol{H}(\hat{s}_j) = \bar{\boldsymbol{H}}(\hat{s}_j)$ at specific expansion points $\hat{s}_j$ in the Laplace-domain. Furthermore, it is possible to match also the derivatives up to a desired order at these expansion points. A third possible method is balanced truncation. The idea is to eliminate those states that require a lot of energy to be reached and have a low observation energy. It is necessary to bring the system into a balanced form so that the reachability and the observability of the states are equivalent.

2.3 Parametric model order reduction

Parametric model order reduction is an extension of classical model order reduction techniques, where parameter dependencies in the system matrices $\boldsymbol{M}(\boldsymbol{p})$, $\boldsymbol{D}(\boldsymbol{p})$ and $\boldsymbol{K}(\boldsymbol{p})$ are retained in the reduced order model. In mechanical systems, parameterization can e.g. be used to vary the geometry of the structure or material properties. In the special case, where the parameter dependence can be expressed in an affine form

$$\boldsymbol{K}(\boldsymbol{p}) = \boldsymbol{K}_0 + \sum_{j=1}^{J} w_j(\boldsymbol{p})\boldsymbol{K}_j \tag{5}$$

with weighting functions $w_j(\boldsymbol{p}) : \mathbb{R}^d \to \mathbb{R}$ depending on the parameter vector $\boldsymbol{p} \in \mathbb{R}^d$ and constant matrices $\boldsymbol{K}_j \in \mathbb{R}^{N\times N}$, projection-based model order reduction can be applied. The resulting reduced

order parametric stiffness matrix

$$\boldsymbol{K}_{\mathrm{red}}(\boldsymbol{p}) = \boldsymbol{V}^{\mathsf{T}}\boldsymbol{K}(\boldsymbol{p})\boldsymbol{V} = \underbrace{\boldsymbol{V}^{\mathsf{T}}\boldsymbol{K}_0\boldsymbol{V}}_{\boldsymbol{K}_{\mathrm{red},0}} + \sum_{j=1}^{J} w_j(\boldsymbol{p}) \underbrace{\boldsymbol{V}^{\mathsf{T}}\boldsymbol{K}_j\boldsymbol{V}}_{\boldsymbol{K}_{\mathrm{red},j}} \tag{6}$$

comprises the same weighting functions $w_j(\boldsymbol{p}) \in \mathbb{R}$ as the full order model in Equation (5) and reduced constant matrices $\boldsymbol{K}_{\mathrm{red},j} \in \mathbb{R}^{n\times n}$. The reduced mass and damping matrices are derived equivalently. The subspace $\mathcal{V}$ and hence the reduction matrix $\boldsymbol{V}$ must be chosen such that the system dynamics for any parameter vectors $\boldsymbol{p} \in \mathcal{P}$ is covered by the reduced order model. Different approaches for parametric model order reduction are explained e.g. in [8, 9]. This publication uses a global approach, where multiple reduction matrices $\widetilde{\boldsymbol{V}}(\hat{\boldsymbol{p}}_{(k)}) \in \mathbb{R}^{N\times n_k}$ are combined to a global reduction matrix

$$\boldsymbol{V} = \begin{bmatrix} \widetilde{\boldsymbol{V}}(\hat{\boldsymbol{p}}_{(1)}) & \widetilde{\boldsymbol{V}}(\hat{\boldsymbol{p}}_{(2)}) & \dots & \widetilde{\boldsymbol{V}}(\hat{\boldsymbol{p}}_{(K)}) \end{bmatrix} \in \mathbb{R}^{N\times\sum n_k}. \tag{7}$$

Each individual reduction matrix is obtained by applying model order reduction as explained in Section 2.2 at a specific parameter point $\hat{\boldsymbol{p}}_{(k)} \in \mathcal{P}$. The subscript in brackets combined with a hat over the parameter $\hat{\bullet}_{(k)}$ always denotes the k-th sample of the parameter. Often a singular value decomposition is additionally applied to the reduction matrix to remove some of the less important columns and to further reduce the order of the reduced system.

2.4 Error measures for system comparison

In this contribution, different error measures are used to compare two models. The coefficient of determination

$$R^2(f_i) = 1 - \frac{\sum_{k=1}^{K} \left(f_{1,i}(\hat{\boldsymbol{p}}_{(k)}) - f_{2,i}(\hat{\boldsymbol{p}}_{(k)})\right)^2}{\sum_{k=1}^{K} \left(f_{1,i}(\hat{\boldsymbol{p}}_{(k)}) - \bar{f}_{1,i}\right)^2}, \tag{8}$$

see e.g. [10], measures how well the i-th eigenfrequency of the second system $f_{2,i}$ fits the i-th eigenfrequency of the first model $f_{1,i}$. It returns 1 for a perfect fit and 0 if the eigenfrequencies are uncorrelated. By $\bar{f}_{1,i}$, the mean value of the eigenfrequencies of the first model is indicated.

The models can also be compared in the frequency domain by calculating the relative frequency response error

$$\varepsilon_{\mathrm{rel}}(\mathrm{i}\omega, \boldsymbol{p}) = \frac{\|\boldsymbol{H}_1(\mathrm{i}\omega, \boldsymbol{p}) - \boldsymbol{H}_2(\mathrm{i}\omega, \boldsymbol{p})\|_{\mathrm{F}}}{\|\boldsymbol{H}_1(\mathrm{i}\omega, \boldsymbol{p})\|_{\mathrm{F}}}. \tag{9}$$

Here, $\|\bullet\|_{\mathrm{F}}$ denotes the Frobenius norm. Equation (9) can be integrated over the frequency range of interest $[\omega_{\min}; \omega_{\max}]$ to get a scalar value of the frequency response error over all frequencies

$$\bar{\varepsilon}(\boldsymbol{p}) = \frac{\sqrt{\int_{\omega_{\min}}^{\omega_{\max}} \|\boldsymbol{H}_1(\mathrm{i}\omega, \boldsymbol{p}) - \boldsymbol{H}_2(\mathrm{i}\omega, \boldsymbol{p})\|_{\mathrm{F}}^2 \,\mathrm{d}\omega}}{\sqrt{\int_{\omega_{\min}}^{\omega_{\max}} \|\boldsymbol{H}_1(\mathrm{i}\omega, \boldsymbol{p})\|_{\mathrm{F}}^2 \,\mathrm{d}\omega}}. \tag{10}$$

A further possibility to compare two systems is to compare the eigenmodes $\boldsymbol{\varphi}$ using the Modal Assurance Criterion

$$\mathrm{MAC}_{i,j}(\boldsymbol{p}) = \frac{\left(\boldsymbol{\varphi}_{1,i}(\boldsymbol{p})^{\mathsf{T}}\boldsymbol{\varphi}_{2,j}(\boldsymbol{p})\right)^2}{\left(\boldsymbol{\varphi}_{1,i}(\boldsymbol{p})^{\mathsf{T}}\boldsymbol{\varphi}_{1,i}(\boldsymbol{p})\right)\left(\boldsymbol{\varphi}_{2,j}(\boldsymbol{p})^{\mathsf{T}}\boldsymbol{\varphi}_{2,j}(\boldsymbol{p})\right)} \tag{11}$$

which is explained in [11]. The i-th eigenmode of the first system is equal to the j-the eigenmode of the second model if $\mathrm{MAC}_{i,j}(\boldsymbol{p}) = 1$ and both modes are orthogonal for $\mathrm{MAC}_{i,j}(\boldsymbol{p}) = 0$.

These error measures are used in two different ways. In Section 3, they are used to compare results obtained from a simulation in Ansys with results from the parameterized Matlab model to validate the parameterization. The same measures are used in Section 4 to compare the reduced parameterized Matlab model with the full parameterized Matlab model.

3 PARAMETERIZATION OF THE ADAPTIVE HIGH-RISE BUILDING

This section describes the non-parametric model of the building, a sensitivity analysis is applied to identify influential parameters, and the parameterized system matrices are constructed using a regression model. The aim is to develop a model which provides a good representation in the frequency range up to 20 Hz, because this is the frequency range that can be controlled by the actuators. Using this parameterized model, it is not necessary to use a finite element software again in each iteration step during the parameter identification. The desired parameter vector values only have to be inserted into the parameterized system matrices. As a consequence, no communication and pre-processing with the finite element software is necessary anymore.

3.1 System description of the adaptive building

Figure 1 shows the finite element model of the structure. The model is currently implemented in Ansys [12]. The entire bearing structure of the adaptive building is made of steel. The outer vertical frame (i.e. sectors 1 to 5) is modeled as a hollow rectangle with BEAM188 elements. Different cross sections, which are also realized in the same way in the real building, are shown in different colors in Figure 1. The remaining structure (sectors 6 to 8) is modeled with LINK180 elements. The material properties are described by the Young's modulus E_{v} and the density ρ_{v} for the vertical frame (sectors 1 to 5), E_{d} and the density ρ_{d} for the diagonal bars (sectors 6 and 8) and E_{h} and the density ρ_{h} for the horizontal bars (sector 7). The resulting model has $N = 296$ degrees of freedom. The currently implemented model also includes Rayleigh damping $\boldsymbol{D} = \alpha\boldsymbol{M} + \beta\boldsymbol{K}$ with $\alpha = 0.01$ and $\beta = 0.001$.

3.2 Sensitivity analysis

In a parameter identification process of a structural model, sometimes plenty of parameters are used and varied during the identification. For the given model, material parameters such as the density and the Young's modulus are possible, but also geometric parameters are worth considering. In parameter identification, it is sometimes not necessary to identify the real parameter values of the structure but to find some parameter values such that the system behavior of the model is as close as possible to the system behavior of the real structure. The system behavior can be described by eigenmodes and eigenfrequencies or by the system response in the time or frequency domain. Considering all possible parameters leads to a high-dimensional parameter space which is hard to handle in the identification

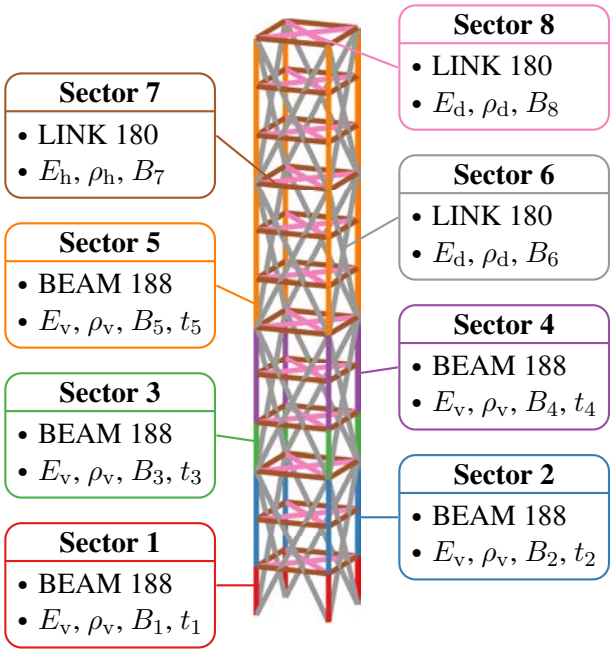

Figure 1: Finite element model of the building with different colors for different parameterization sectors.

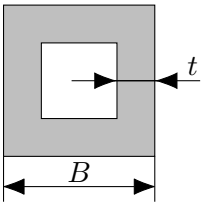

Figure 2: Quadratic cross section of the beam elements with width B and thickness t.

process. Furthermore, the computation of a suitable subspace for the parametric model order reduction that can represent the entire parameter space is much more challenging. For this reason, it is better to restrict the dimension of the parameter space in advance by using only the most influential parameters. A local sensitivity analysis using the Pearson Correlation Coefficient, see e.g. [13],

$$R(p_j, f_k) = \frac{1}{H-1} \sum_{h=1}^{I} \left(\frac{(p_j)_{(h)} - \bar{p}_j}{\sigma_{p_j}} \right) \left(\frac{(f_k)_{(h)} - \bar{f}_k}{\sigma_{f_k}} \right) \tag{12}$$

is conducted to measure the correlation between the j-th parameter p_j and the k-th eigenfrequency f_k. The definition contains the arithmetic mean $\bar{p}_j$ and $\bar{f}_k$, the standard deviation σ_{p_j} and σ_{f_k} as well as the number of simulated samples H. For each beam sector, i.e. sector 1 to 5, the width B_i and the thickness t_i of the cross section, see Figure 2, are taken into account. The link sectors 6, 7 and 8 are parameterized only by their individual width B_i. The material properties described in the previous section are also considered. Other parameters such as the length of the element or the Poisson ratios are kept constant. This gives a total of 19 parameters. In total, $H = 200$ parameter vector samples are chosen in a range of $\pm 2\,\%$ around their nominal value using a Latin Hypercube sampling. For the analysis, the first 15 eigenfrequencies are considered as they cover the required frequency range. The resulting correlation is shown in Figure 3. To get a better overview over the most relevant parameters, the pie chart in Figure 4 shows the absolute correlation coefficient averaged over the frequency range of interest. The colors in the pie chart correspond to the colors in Figure 1. The indices correspond to the numbers of the sector. As the colors only distinguish between the different cross-sections, but not between the material properties,

the color yellow is also introduced for the identical material properties of sectors 1-5. The pie chart shows that the eigenfrequencies are mainly influenced by nine parameters. The influence of the other parameters is so small that they will not be considered in the further analysis. This first step does not change the matrices but identifies the most important parameters which should be kept as variables in the reduced order parametric model developed in the following sections.

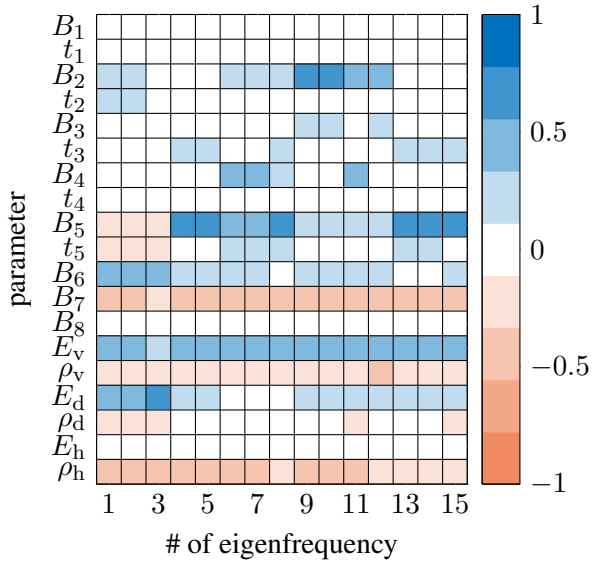

Figure 3: Correlation coefficient between the parameters and the eigenfrequencies.

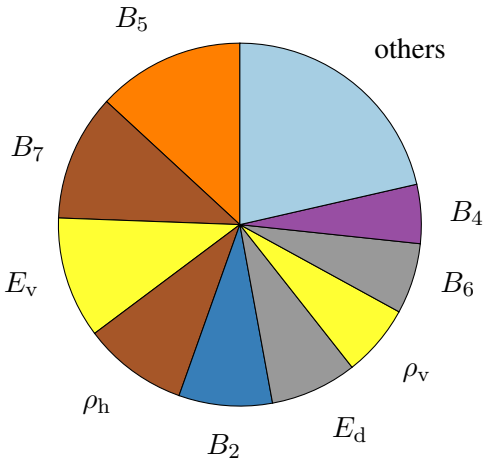

Figure 4: Mean absolute correlation coefficient averaged over all frequencies.

3.3 Parameterized model of the adaptive building

The next step is to identify the dependency of the system matrices on the important parameters identified in the previous section to built the parameterized model. From the finite element theory, e.g. [14], the dependence of the element matrices on the parameters is known. For each beam sector, these information can be used to formulate the weighting functions in the affine stiffness matrix from Equation (5), which can then be formulated as

$$\boldsymbol{K}(\boldsymbol{p}) = \widetilde{\boldsymbol{K}}_0 + \underbrace{EA\widetilde{\boldsymbol{K}}_1}_{\text{axial}} + \underbrace{EI_\mathrm{y}\widetilde{\boldsymbol{K}}_2 + EI_\mathrm{z}\widetilde{\boldsymbol{K}}_3}_{\text{bending}} + \underbrace{GI_\mathrm{p}\widetilde{\boldsymbol{K}}_4}_{\text{torsion}} + \underbrace{GA\widetilde{\boldsymbol{K}}_5}_{\text{shear}} \tag{13}$$

with the cross section area A, the second moments of area I_y and I_z, the polar moment of inertia I_p and the shear modulus G. Due to the symmetry of the cross section, I_y and I_z are equal and can be expressed by I. With $I_\mathrm{p} = I_\mathrm{y} + I_\mathrm{z}$ and $G = \frac{E}{2(1+\nu)}$, and assuming the Poisson ratio ν as constant, since its variation is not considered in this contribution, Equation (13) simplifies to $\boldsymbol{K}(\boldsymbol{p}) = \boldsymbol{K}_0 + EA\boldsymbol{K}_1 + EI\boldsymbol{K}_2$.

In this study, a regression model is used to find the unknown constant matrices $\boldsymbol{K}_j$ with $j \in \{0, 1, 2\}$ in the affine representation. The resulting basis function for the regression model is

$$\boldsymbol{x}(\hat{\boldsymbol{p}}_{(h)})^\mathsf{T} = \begin{pmatrix} 1 & \hat{E}_{(h)}\hat{A}_{(h)} & \hat{E}_{(h)}\hat{I}_{(h)} \end{pmatrix}, \tag{14}$$

where $\hat{\bullet}_{(h)}$ stands for a specific value of the corresponding parameter, and $\hat{A}_{(h)}$ and $\hat{I}_{(h)}$ depend on the width $\hat{B}_{(h)}$ and thickness $\hat{t}_{(h)}$ of the cross-section. The resulting regression is

$$\underbrace{\begin{pmatrix} k_{k,l}(\hat{\boldsymbol{p}}_{(1)}) \\ k_{k,l}(\hat{\boldsymbol{p}}_{(2)}) \\ \vdots \\ k_{k,l}(\hat{\boldsymbol{p}}_{(H)}) \end{pmatrix}}_{\boldsymbol{k}_{k,l}^{\mathrm{Ansys}} \in \mathbb{R}^H} = \underbrace{\begin{pmatrix} \boldsymbol{x}(\hat{\boldsymbol{p}}_{(1)})^{\mathsf{T}} \\ \boldsymbol{x}(\hat{\boldsymbol{p}}_{(2)})^{\mathsf{T}} \\ \vdots \\ \boldsymbol{x}(\hat{\boldsymbol{p}}_{(H)})^{\mathsf{T}} \end{pmatrix}}_{\boldsymbol{X} \in \mathbb{R}^{H \times J+1}} \underbrace{\begin{pmatrix} k_{k,l,0} \\ k_{k,l,1} \\ \vdots \\ k_{k,l,J} \end{pmatrix}}_{\boldsymbol{k}_{k,l} \in \mathbb{R}^{J+1}}, \tag{15}$$

where $k_{k,l}(\hat{\boldsymbol{p}}_{(h)})$ is the (k,l)-th entry of the stiffness matrix obtained from Ansys with the parameter sample $\hat{\boldsymbol{p}}_{(h)}$ and $\boldsymbol{k}_{k,l,j}$ is the entry in row k and column l of the unknown matrix $\boldsymbol{K}_j$. Since the parameters that have little influence on the eigenfrequencies are kept constant, see Section 3.2, some columns of $\boldsymbol{X}$ are also constant and can be neglected. In order to avoid an under-determined system of equations, it is important, that the number of samples H for the regression is always larger or equal to the number of matrices in the affine representation J. The Moore–Penrose pseudoinverse $\boldsymbol{X}^{+} = (\boldsymbol{X}^{\mathsf{T}}\boldsymbol{X})^{-1}\boldsymbol{X}^{\mathsf{T}}$ is used to calculate the unknowns $\boldsymbol{k}_{k,l} = \boldsymbol{X}^{+}\boldsymbol{k}_{k,l}^{\mathrm{Ansys}}$. The procedure is repeated for every sector shown in Figure 1 and finally, the global stiffness matrix is assembled. Since link elements do not include bending, shear and torsion, see [12], the relevant ansatz for them is only $\boldsymbol{K}(\boldsymbol{p}) = \boldsymbol{K}_0 + EA\boldsymbol{K}_1$. The parameterized mass matrix is calculated analogously by replacing the Young's modulus with the density which results in the approaches $\boldsymbol{M}(\boldsymbol{p}) = \boldsymbol{M}_0 + \rho A\boldsymbol{M}_1 + \rho I\boldsymbol{M}_2$ for beams and $\boldsymbol{M}(\boldsymbol{p}) = \boldsymbol{M}_0 + \rho A\boldsymbol{M}_1$ for the link elements.

3.4 Validation of the parameterized model

Some effects, such as the shear correction factor or locking, which may cause other important dependencies than those selected in the basis function, that are not included in the regression model. It is therefore even more important to validate the implemented parameterized model. If the ansatz functions are correctly selected in the regression, the correct system matrices can be calculated with the parametric model for any possible parameter vector. However, for the parametric model order reduction performed later, it is advantageous to restrict the possible parameter space. The feasible parameter space $\mathcal{P}$ includes all parameter vectors within $\pm 20\,\%$ of the nominal value. Figure 5 shows the range of the relative frequency response error from Equation (9) between Ansys and the parameterized Matlab model for 100 randomly selected parameter samples in the parameter space. The fact that the error is consistently below $0.5\,\%$ shows that the parameterization provides very good results over the entire frequency range and that no additional effects need to be taken into account. Additionally, the coefficient of determination introduced in Equation (8) is larger than 0.999 for all eigenfrequencies, which also indicates a very good approximation.

Instead of doing pre-processing steps in Ansys and to transfer the data between Ansys and Matlab, which would be necessary with the Ansys model, the parametric model allows to obtain the system matrices of a specific parameter sample by simply inserting this parameter sample into the weighting functions of the parameterized system matrices in Equation (5). As a consequence, the computational time to get the system matrices is reduced from $1.45\,\mathrm{s}$ in Ansys to $0.0023\,\mathrm{s}$ with the parameterized full order model. This enables an efficient system evaluation during the online phase of the parameter identification, where possibly hundreds of system evaluations at different parameter samples have to be

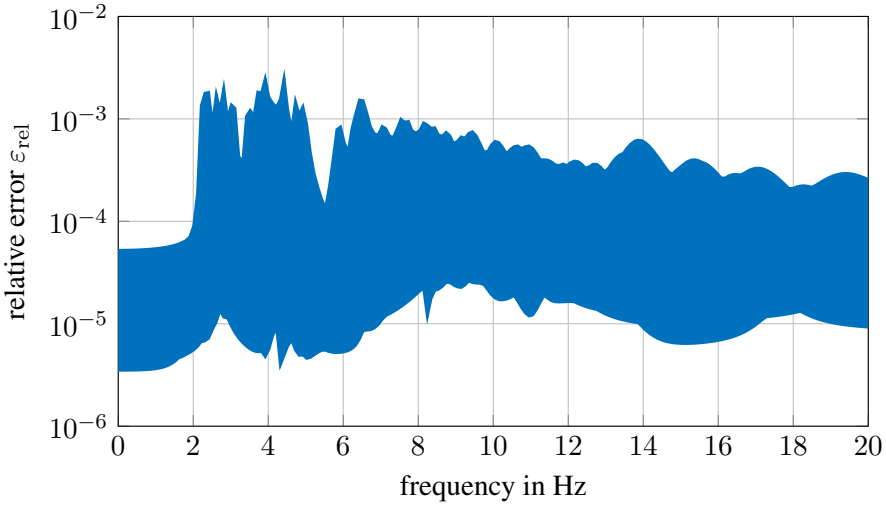

Figure 5: Relative error (Equation (9)) in the frequency domain between the full order Ansys model and the parameterized full order Matlab model for 100 randomly selected parameter samples.

done. As the parameterized model is faster to evaluate and has a high accuracy in the required parameter and frequency domain, from now on every calculation requiring evaluation of the full order model is performed using the parameterized full order model. The Ansys model is not necessary anymore.

4 MODEL ORDER REDUCTION OF THE PARAMETERIZED MODEL

In order to reduce not only the time required to evaluate the system matrices at specific parameter samples, but also the computational time for transient simulations or eigenvalue analysis, which depend, among other things, on the system dimension, parametric model order reduction is applied. The goal of this section is to find a subspace $\mathcal{V}$ such that the approximation error between the parameterized full order model and the parameterized reduced order model becomes sufficiently small in the given parameter space $\mathcal{P}$.

First of all, different linear model order reduction techniques are applied to find an appropriate reduction method. At this stage, it is not a global parametric reduction, but only a linear model order reduction. This means, that each reduction is done at the same parameter point. The parameterized model is evaluated at this parameter point and a linear model order reduction according to Section 2.2 is applied. These two models are compared in Figure 6 using the mean relative error (Equation (10)) integrated over a frequency range from 0 Hz to 20 Hz for moment matching, modal truncation, and balanced truncation for different reduction orders n. It can be seen that balanced truncation provides the best results for nearly all reduction orders. The reduction order is chosen such that the mean relative reduction error (Equation (10)) is lower than 0.01 resulting in a reduction order of 23. It is not guaranteed that a reduction order of 23 is sufficient in the whole parameter domain. However, it is shown in the following that choosing a suitable number of expansion points in the parameter domain enables a good approximation in the entire frequency and parameter space.

As already explained in Section 2.3, the global reduction basis for the parameterized system needs multiple expansion points in the parameter domain. Figure 7 shows the relative reduction error for

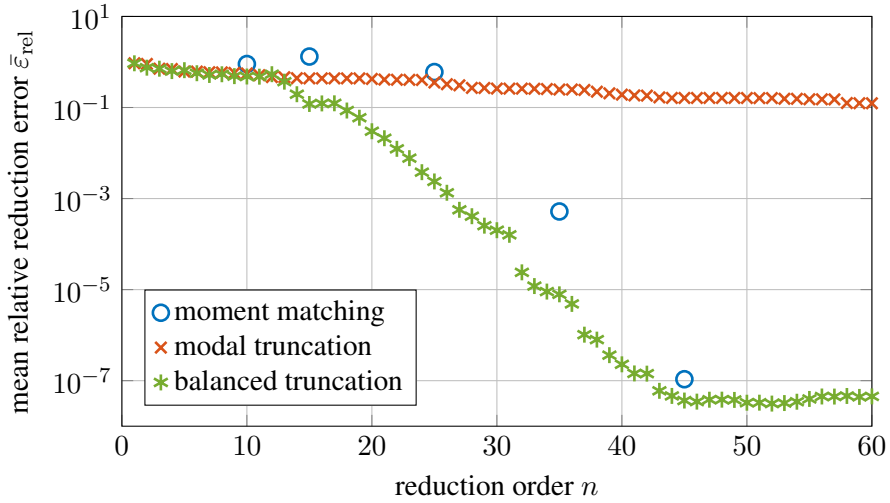

Figure 6: Mean relative reduction error (Equation (10)) for different reduction orders and different reduction methods.

different numbers of expansion points, to find out the necessary number of expansion points. Each reduction is evaluated on 100 samples in the parameter space. With an increasing number of parameter expansion points, the reduction error between the full order parameterized model and the parameterized reduced order model becomes smaller. The reduction error is always smaller than 0.01 for four expansion points indicating a sufficient approximation. Having an individual reduction order of 23, concatenating these four individual reduction matrices to a global reduction matrix as explained in Equation (7) results in a reduced order model with $4 \cdot 23 = 92$ degrees of freedom. A further validation of the reduced

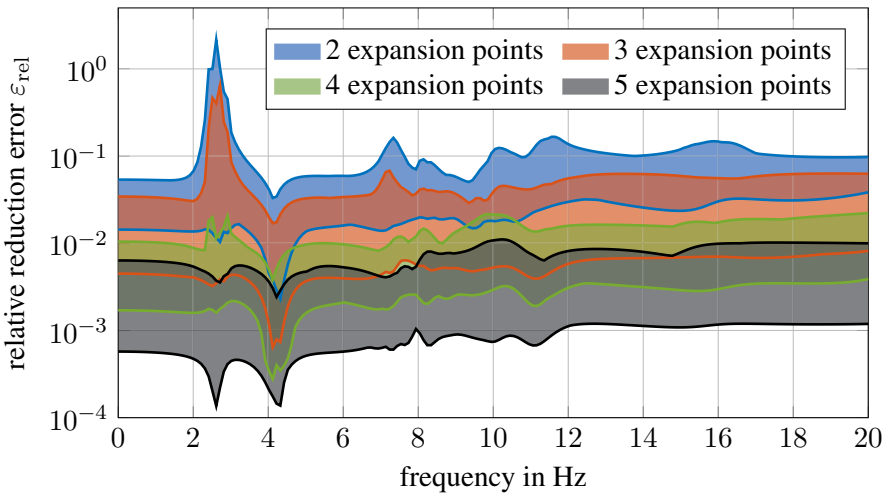

Figure 7: Comparison of the number of expansion points in the parameter domain using the relative reduction error (Equation (9)) between the full order parameterized model and the reduced order parameterized model.

order model is done using the Modal Assurance Criterion introduced in Equation (11). Figure 8 shows the Modal Assurance Criterion for a randomly selected parameter sample in the parameter space. It reveals the close match between the full order parameterized model and the parameterized reduced order model. The axis labels also show that there is good agreement between the eigenfrequencies of the two models. Due to the limited space in this contribution, only one parameter sample is shown. However, the approximation of the eigenvalues and eigenmodes is similarly good in the entire parameter space. The evaluation of the frequency response of the reduced order model needs only $0.128\,\mathrm{s}$ in contrast to $0.643\,\mathrm{s}$ for the full order model. The calculation time for the eigenfrequencies is reduced from $0.0044\,\mathrm{s}$ to $0.0025\,\mathrm{s}$. Combined with the time saved by parameterization in Section 3, this results in a significant reduction in the online computation time.

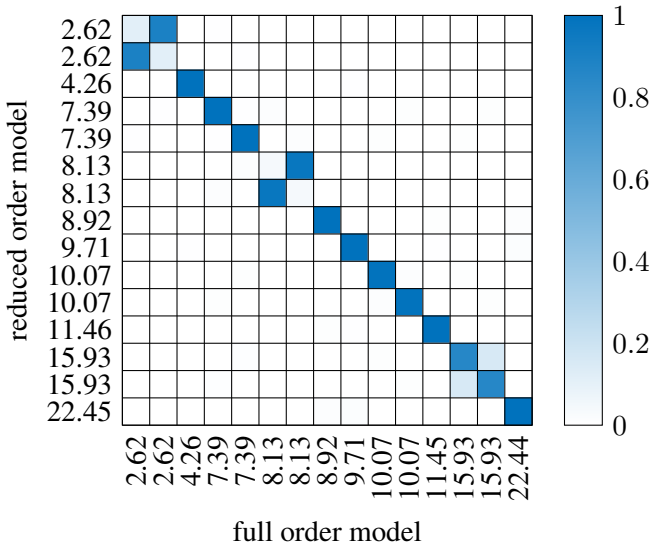

Figure 8: Comparison of the mode shapes of the reduced order parameterized model and the full order parameterized model with the Modal Assurance Criterion (Equation (11)) at a random parameter sample in the parameter space.

5 CONCLUSION

In this paper, a parameterized finite element model of a high-rise building was derived. With the help of a sensitivity analysis, the number of design parameters was reduced from 19 to nine which has benefits for the parametric model order reduction and the parameter identification. Finite element beam theory and regression was used to identify the parameter dependency of the system matrices. With the help of the parameterized full order system matrices, a balanced truncation based parametric model order reduction was applied. Although the offline phase involved a high computational effort, this method has advantages over the non-parameterized model in the online phase because solely the reduced model is used in the online phase and computation time for pre-processing can be eliminated, which results in a faster evaluation of the system matrices and an acceleration of the calculation of the transfer function or eigenvalues.

6 ACKNOWLEDGEMENT

This project is funded by the Deutsche Forschungsgemeinschaft (DFG, German Research Foundation) – Project-ID 279064222 – SFB 1244, "Adaptive skins and structures for the built environment of tomorrow" with the projects B01, B02, and B04. This support is highly appreciated.

References

[1] United Nations, International Energy Agency, "Global status report for buildings and construction 2019," *UN Enviroment programme*, vol. 224, 2019.

[2] L. Blandini, W. Haase, S. Weidner, M. Böhm, T. Burghardt, D. Roth, O. Sawodny, and W. Sobek, "D1244: Design and construction of the first adaptive high-rise experimental building," *Frontiers in Built Environment*, vol. 8, 2022.

[3] O. C. Zienkiewicz, R. L. Taylor, and J. Z. Zhu, *The Finite Element Method – Its Basis & Fundamentals*. Oxford: Butterworth-Heinemann, 2005.

[4] K.-J. Bathe, *Finite Element Procedures*. Upper Saddle River: Prentice Hall, 2014.

[5] A. Antoulas, *Approximation of Large-Scale Dynamical Systems*. Philadelphia: SIAM, 2005.

[6] P. Benner, M. Ohlberger, A. Cohen, and K. Willcox, *Model Reduction and Approximation. Theory and Algorithms*. SIAM, 2017.

[7] J. Fehr and P. Eberhard, "Error-controlled model reduction in flexible multibody dynamics," *Journal of Computational and Nonlinear Dynamics*, vol. 5, no. 3, pp. 031 005–1–031 005–8, 2010.

[8] P. Benner, S. Gugercin, and K. Willcox, "A survey of projection-based model reduction methods for parametric dynamical systems," *SIAM Review*, vol. 57, no. 4, pp. 483–531, 2015.

[9] M. Baumann, *Parametrische Modellreduktion in elastischen Mehrkörpersystemen*, ser. Dissertation, Schriften aus dem Institut für Technische und Numerische Mechanik der Universität Stuttgart, Vol. 43. Aachen: Shaker Verlag, 2016.

[10] A. G. Asuero, A. Sayago, and A. González, "The correlation coefficient: An overview," *Critical Reviews in Analytical Chemistry*, vol. 36, no. 1, pp. 41–59, 2006.

[11] R. Allemang, "The modal assurance criterion - 20 years of use and abuse," in *Proceedings of the 20th International Modal Analysis Conference, Los Angeles, USA*, 2002, pp. 14–21.

[12] Ansys, *Documentation for Ansys, Release 18.2*, Ansys, Inc., 2018.

[13] D. M. Hamby, "A review of techniques for parameter sensitivity analysis of environmental models," *Environmental Monitoring and Assessment*, vol. 32, pp. 135–154, 1994.

[14] O. C. Zienkiewicz and R. L. Taylor, *The Finite Element Method for Solid and Structural Mechanics*. Oxford: Butterworth-Heinemann, 2005.